COBEM 99
XV Congresso Brasileiro de Engenharia Mecânica
15th Brazilian Congress of Mechanical Engineering
22 - 26 de Novembro de 1999 / November 22 - 26, 1999 Águas de Lindóia, São Paulo,

MICROMECHANICS AND CONTINUUM MODELING OF 3-D CONSTRAINT EFFECTS FOR FRACTURE ASSESSMENTS OF STRUCTURES

Claudio Ruggieri
Department of Naval Architecture and Ocean Engineering, University of São Paulo
São Paulo, SP 05508–900, E-mail: cruggi@usp.br, Brazil

Robert H. Dodds, Jr.
Department of Civil Engineering, University of Illinois at Urbana-Champaign
Urbana, IL 61801, E-mail: r-dodds@uiuc.edu, US

Abstract *– This paper presents a summary of the descriptive (continuum) and predictive (micromechanics incorporating statistics) approaches to characterize constraint effects on cleavage fracture toughness. Discussions emphasize features of the J-Q approach to extend descriptive fracture mechanics using J-Q trajectories. The paper then addresses a local (micromechanics) approach for cleavage fracture based on a probabilistic fracture parameter – the Weibull stress (σ_w). The presentation explores development of a toughness scaling methodology based upon Weibull stress trajectories for different crack configurations which enables assessment of constraint loss in conventional fracture specimens and 3-D cracked solids.*

Key words: *cleavage fracture, constraint, statistical effects, local approach, Weibull stress*

1. INTRODUCTION

Conventional fracture mechanics methodologies to assess unstable cracking behavior (cleavage fracture) of different cracked bodies (i.e., laboratory specimens and engineering structures) rely on the similarity of their respective crack tip stress and deformation fields. Under well-contained near-tip plasticity, a single parameter, such as the linear elastic stress intensity factor, K, and the J-integral (or, equivalently, the crack tip opening displacement, CTOD or δ), uniquely scales the elastic-plastic near-tip fields. To the extent that such one-parameter singular fields dominate over microstructuraly significant size scales (i.e., the fracture process zone of a few CTODs ahead of a macroscopic crack), the parameters K and J (δ) fully describe the local conditions leading to unstable (cleavage) failure. However, fracture testing of ferritic structural steels in the ductile-to-brittle (DBT) transition region consistently reveals a significant effect of specimen geometry and loading mode (bending *vs.* tension) in measured cleavage toughness values (i.e., the critical parameters $K_{\rm Ic}$, J_c, δ_c). Moreover, well within the transition region, strong statistical effects on fracture toughness arise due to variability of cleavage resistance at microstructural level; such statistical effects cause large scatter on measured toughness values. Figure 1 provides illustrative data for typical structural steels tested in the DBT transition region (Toyoda et al., 1991; Wiesner et al., 1996). which display large amount of scatter in J_c-values. In particular, Fig. 1(a) clearly shows significant elevations in the measured values of cleavage fracture toughness for shallow crack SE(B) specimens. This *apparent*

increased toughness of structural steels in service conditions has enormous practical implications in defect assessment procedures, particularly repair decisions and life extension programs of in-service structures. Moreover, the large amount of scatter, coupled with specimen geometry effects, greatly complicates the interpretation of toughness data to define meaningful values for applications in fracture assessments of structures.

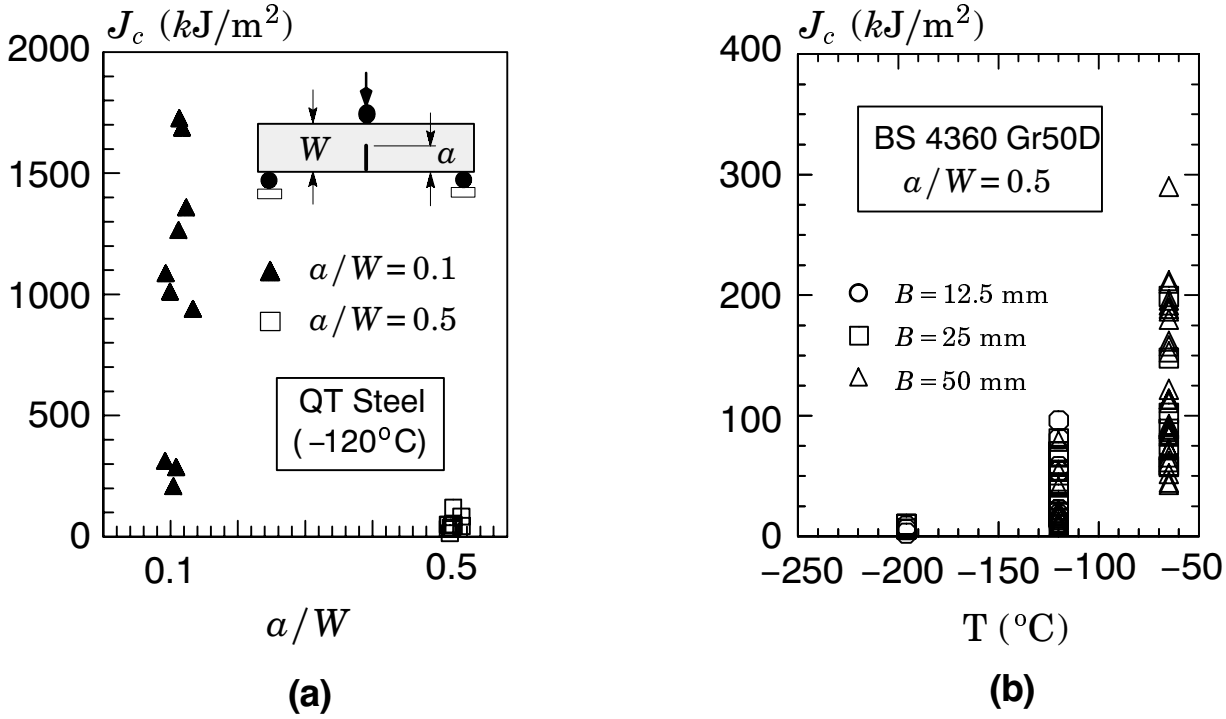

Figure 1 *(a) Experimental cleavage fracture toughness data (SE(B) test results) for a quenched and tempered (QT) steel at –120°C (Toyoda et al., 1991). (b) Measured toughness data for a structural BS 4360 steel (Wiesner et al., 1996) (deep notch SE(B) specimens with varying thickness and $a/W = 0.5$).*

The marked differences of J_c-values for shallow crack and deep crack specimen geometries exhibited by the plots shown in Fig. 1(a) underly the loss of one-to-one correspondence between J and the elastic-plastic crack-tip fields. This loss of uniqueness, most often termed as *loss of constraint*, produces the increase of toughness values in shallow crack bend specimens and tension loaded geometries. The issue of constraint loss for a *finite* cracked body is conveniently addressed by considering a reference constraint level associated with a reference crack-tip field. Differences in levels of stress triaxiality ahead of the crack front under increased remote loading (as measured by J) for a *reference* field and for the near-tip fields of the finite cracked body quantifies the "relative" constraint for the finite body. While there is no unique choice for the reference field, it proves convenient to adopt the high triaxiality small scale yielding (SSY) fields as the reference solution. The SSY fields are easily constructed from the modified boundary layer (MBL) formulation (Larsson and Carlsson, 1973) to a single-ended crack in an infinite body. Computational procedures to obtain the necessary fields generally employ finite element analyses incorporating general material response under small geometry changes (SGC) or large geometry changes (LCG) – see details of the numerical implementation in Trovato and Ruggieri (1999). Within this framework, the differences in the *actual* finite-body field and the reference SSY field quantify the extent of large scale yielding (LSY) that develops as deformation progresses. At increasing loads in the finite body, the initially strong SSY fields gradually diminish as crack-tip plastic zones increasingly merge with the global bending plasticity on the nearby traction free boundaries. The phenomenon of constraint loss requires larger J-values in the finite body to generate a highly stressed region ahead of crack tip sufficient to trigger cleavage. Consequently, once SSY conditions no longer apply, the near-tip stresses (and

strains) that develop ahead of a macroscopic crack cannot be described *uniquely* by J (or, equivalently, by K or CTOD).

The above arguments that a single parameter might not suffice to characterize the near-tip behavior of cracked geometries under LSY conditions motivated the development of two-parameter fracture theories. Under fixed loading, such methodologies assume a separable form for the actual cracked-body fields in a high triaxiality fields (such as the SSY field) and a *constant* field which quantifies the level of crack tip stress triaxiality. These research efforts proceed along essentially two lines: (1) the J-T methodology building upon the elastic T-stress (see review by Parks (1992)), and (2) the J-Q methodology developed by O'Dowd and Shih (1991, 1992) building upon the hydrostatic parameter Q. Both frameworks characterize families of self-similar fields which describe crack tip fracture states in the full range of high and low triaxiality: in each one, J sets the size scale over which large stresses and strain develop while the second parameter (T or Q) scales the near-tip distribution relative to the reference stress state.

While the J-T and J-Q approaches are equivalent under well-contained near-tip plastic deformation, the elastic T-stress become undefined under fully-yielded conditions as the elastic near-tip fields upon which T is derived no longer apply. In contrast, the Q-parameter continues to characterize the evolution of near-tip stress triaxiality over a wider range of crack-tip plasticity associated with a wide variety of crack configurations under general loading conditions. A concept of *toughness locus* for a specific material and temperature then emerges in connection with a J-Q driving force trajectory for each crack geometry; the toughness locus for the material is constructed upon determining the Q-value at fracture which corresponds to each measured J_c-value (O'Dowd and Shih, 1992; Dodds et al., 1993). However, the large number of fracture specimens and temperatures needed to construct the J-Q toughness locus greatly complicates the direct implementation of this approach to fracture assessments as does the application of the method (which derives from a 2-D framework) to fully 3-D crack geometries. Moreover, such models do not address the strong statistical effects on cleavage fracture in the DBT region neither do they provide a means to *predict* the effects of constraint and prior ductile tearing on toughness.

The above limitations of continuum (*descriptive*) fracture mechanics approaches to characterize the fracture behavior of fully yielded crack geometries motivated the development of micromechanics models based upon a probabilistic interpretation of the fracture process (most often referred to as *local approaches*). Attention has been primarily focused on probabilistic models incorporating weakest link statistics to describe material failure caused by stress-controlled transgranular cleavage. By coupling macroscopic measures of fracture toughness (J, CTOD) with micromechanics models for material failure ahead of the crack tip, researchers endeavour to *predict*, rather than correlate, constraint effects on fracture toughness. The seminal work of Beremin (1983) provides the basis for establishing a relationship between the microregime of fracture and macroscopic crack driving forces (such as the J-integral) by introducing the Weibull stress (σ_w) as a probabilistic fracture parameter. Retaining contact with conventional approaches, this fracture parameter conveniently characterizes macroscopic fracture behavior for a wide range of loading conditions and crack configurations. A key feature of the Beremin approach is that σ_w follows a two-parameter Weibull distribution (Mann et al., 1974) in terms of the Weibull modulus, m, and the scale parameter, σ_u. Further idealization postulates that parameter m represents a material property in this model (Mudry, 1987) which provides a means to correlate fracture toughness for varying crack configurations under different loading/temperature conditions. When implemented in a finite element code, the Beremin model predicts the evolution of the Weibull stress with applied load to define conditions leading to (local) material failure. More recent efforts in this area have focused on developing transferability models for cleavage fracture toughness based upon the Beremin's Weibull stress. Minami et al. (1992), Ruggieri et al. (1995), assess effects of specimen thickness and crack length on elastic-plastic fracture toughness (J_c, δ_c). Further studies by Ruggieri and Dodds (R&D) (1996, 1997, 1998) generalize the Weibull stress for stationary and growing cracks to include the effects of loss of constraint and ductile tearing on macroscopic fracture toughness.

The objectives of this paper focus on a summary of the descriptive (continuum) and predictive (micromechanics incorporating statistics) approaches to characterize constraint effects on cleavage fracture toughness. Discussions emphasize features of the J-Q approach to extend descriptive fracture mechanics using J-Q trajectories. The paper then addresses a local (micromechanics) approach for cleavage fracture based on the Weibull stress. The presentation explores development of a toughness scaling methodology based upon the Weibull stress trajectories for different crack configurations which enables assessment of constraint loss in conventional fracture specimens.

2. TWO-PARAMETER CHARACTERIZATION: THE J-Q METHODOLOGY

2.1 J-Q Theory

The characteristic feature emerging from a multi-parameter description of the (stationary) elastic-plastic crack tip fields in homogeneous materials is the use of a scalar parameter to quantify the magnitude of these fields. Here, the J-integral sets the size scale over which high stresses develop while the second parameter (the elastic T-stress or the hydrostatic Q-parameter) quantifies the level of stress triaxiality at distances of a few CTODS ahead of the crack tip. In particular, the J-Q description of mode I, plane strain crack tip fields derives from consideration of a modified boundary layer (MBL) formulation [3] in which the remote tractions are given by the first two-terms of Williams' linear elastic solution (Williams, 1957)

$$\sigma_{ij} = \frac{K_{\mathrm{I}}}{\sqrt{2\pi r}} f_{ij}(\theta) + T\delta_{1i}\delta_{1j} \ . \tag{1}$$

Here r and θ are polar coordinates centered at the crack tip with $\theta = 0$ corresponding to a line ahead of the crack and $K_{\mathrm{I}} = \sqrt{EJ/(1-\nu^2)}$, E is Young's modulus, ν is Poisson's ratio and f_{ij} are dimensionless functions of θ. Crack tip fields differing in stress triaxiality are generated by varying the non-singular stress, T, parallel to the crack plane (which does not affect the value of J). From dimensional considerations, these fields can be represented by a family of self-similar fields parameterized by the load parameter T/σ_0 which provides a convenient measure of near-tip stress triaxiality such as, for example, when assessing effects of specimen geometry on crack tip constraint. However, the general applicability of T under fully yielded conditions become elusive since the elastic solution given by (1), upon which the T-stress is defined, is an asymptotic solution which is increasingly violated as plastic flow progresses beyond well-contained near-tip yielding.

The above limitations motivated O'Dowd and Shih (OS) (1991, 1992) to propose an *approximate* two-parameter description for the elastic-plastic crack tip fields based upon a triaxiality parameter more applicable under LSY conditions for materials with elastic-plastic response described by a power hardening law given by $\epsilon/\epsilon_0 \propto (\sigma/\sigma_0)^n$. Here, n denotes the strain hardening exponent, σ_0 and ϵ_0 are the reference (yield) stress and strain, respectively. Guided by detailed numerical analyses employing the MBL model OS identified a family of self-similar fields in the form

$$\sigma_{ij} = \sigma_0 \hat{f}_{ij}\left(\frac{r}{J/\sigma_0}, \theta, Q/\sigma_0\right) \ , \tag{2}$$

where the dimensionless second parameter Q defines the amount by which σ_{ij} in fracture specimens differ from the reference SSY solution with $T = 0$.

Limiting attention to the forward sector ahead of the crack tip between the $\mathrm{SSY}_{T=0}$ and the fracture specimen fields, OS showed that $Q\sigma_0$ corresponds effectively to a spatially uniform hydrostatic stress, i.e., the *difference* field relative to a high triaxiality reference stress state

$$\sigma_{ij} = (\sigma_{ij})_{\mathrm{SSY;T=0}} + Q\sigma_0\delta_{1i}\delta_{1j} \ ; \quad |\theta| < \frac{\pi}{2}, \ J/\sigma_0 < r < 5J/\sigma_0 \ . \tag{3}$$

Operationally, Q is defined by

$$Q \equiv \frac{\sigma_{\theta\theta} - (\sigma_{\theta\theta})_{SSY;T=0}}{\sigma_0}, \qquad \text{at } \theta = 0,\ r = 2J/\sigma_0 \tag{4}$$

where finite element analyses containing sufficient mesh refinement to resolve the fields at this length scale provide the finite body stresses. Here, we note that Q is evaluated at $r = 2J/\sigma_0$ for definiteness; however, OS also showed that Q is virtually independent of distance in the range $J/\sigma_0 < r < 5J/\sigma_0$.

Construction of a *J-Q trajectory* follows by the evaluation of Eq. (4) at each stage in loading of the finite body. Again, this procedure imposes no restrictions on models to describe material flow properties or incremental *vs.* deformation plasticity. Large geometry changes (LGC) may be included although values of Q derived from small geometry change (SGC) analyses prove satisfactory in applications which make use of stresses sufficiently outside the near tip blunting region. To incorporate loading rate (i.e., strain rate) effects on material response in the boundary layer model, the $K_I(T=0)$ displacement field is imposed over prescribed time increments.

Figures 2(a) and 2(b) show the J-Q trajectories generated under increased loading at locations over the crack front for plane-sided, deep and shallow notch SE(B) specimens having $W/B = 1$ and $n = 10$ (Nevalainen and Dodds, 1995). Here, W denotes the specimen width and B is the specimen thickness. Q is defined by Eq. (4) at the normalized distance ahead of the crack front given by $r/(J/\sigma_0) = 2$. For the deep notch in Fig. 2 (a), Q-values are positive at low loads (corresponding to the positive elastic T-stress for this geometry) except near the outside surface ($z/(B/2) \gtrsim 0.6$). Over the center portion of the specimen thickness, SSY conditions ($Q \geq 0$) exist *strictly* for deformation levels $b > 140 J_{avg}/\sigma_0$, where b denotes the remaining ligament length and J_{avg} is the average J-value over the crack front; at larger deformations Q takes on negative values. The plane-strain result for this configuration shown in Fig. 2 (a) indicates constraint loss at lower-levels of deformation, $b > 170 J_{avg}/\sigma_0$. The difference between plane-strain and 3-D (centerplane) trajectories increases with continued loading. In contrast, Q-values for the $a/W = 0.1$ configuration reveal an immediate loss of constraint upon loading n Fig. 2 (b). The plane-strain result agrees reasonably well with the 3-D analysis over this portion of the crack front. The global bending field impinges less strongly on the crack-tip fields in the shallow notch geometry. However, no practical size/deformation limit exists to maintain SSY conditions in this specimen; constraint loss occurs upon initial loading (the T-stress is negative for this a/W ratio).

2.2 Fracture Toughness Locus Using *J-Q* Trajectories

Testing of fracture specimens enables construction of *J-Q toughness loci* to characterize cleavage fracture toughness over a range of crack tip stress triaxiality at a fixed temperature in the DBT range (Dodds et al., 1993). Experimentally measured J-values at cleavage fracture are plotted on the trajectories computed by finite element analyses for the specimens, such as those shown in Fig. 3(a). The Q-value at fracture is thus not measured; rather it is inferred by the J controlled location on the appropriate J-Q trajectory. The usual scatter in results observed for multiple tests of the same specimen configuration defines points that lie along the loading trajectory for that specimen. By connecting, separately, the upper-most fracture value on all loading trajectories tested and then the lower-most fracture values, measured envelopes of toughness may be constructed. Utilization of the toughness locus in fracture assessments is illustrated in Fig. 3(b). The driving force curve for a highly constrained geometry (structure A) rises rapidly in the J-Q space. Consequently, cleavage fracture occurs when it intersects the failure locus for cleavage. In contrast, a low constraint geometry (structure B) induces a gradually rising driving force so that ductile tearing is the likely event at overload.

The success in correlating fracture conditions across different crack geometries/loading modes of the same material depends on how well the experimental toughness locus represents the *actual* fracture process in J-Q space (see Fig. 3). The experimental determination of a toughness locus can become very costly, requiring considerable material and testing time, especially if toughness data are needed for varying test temperatures. Additional complications re-

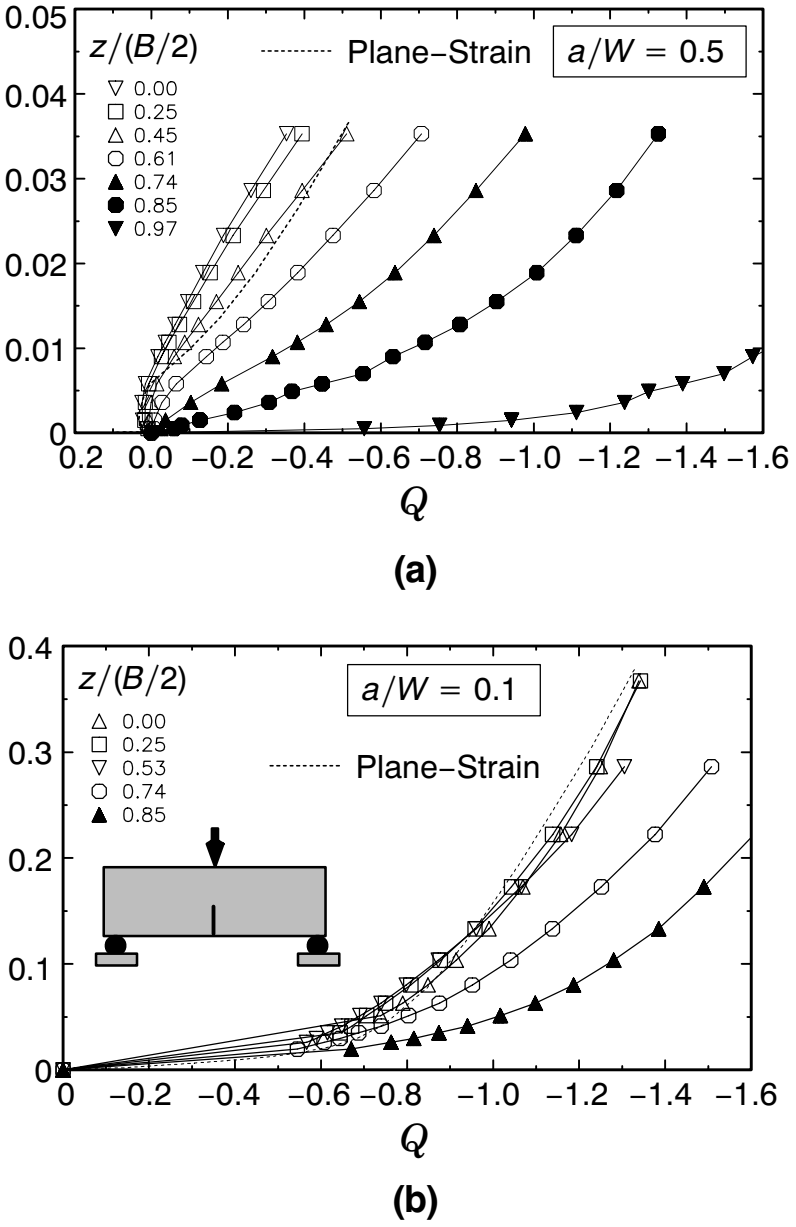

Figure 2 *J-Q trajectories for plane-sided, SE(B) specimens with W/B = 1 at different crack front locations, z/(B/2) (z is the thickness coordinate). The strain hardening exponent in all analyses is n = 10 (Nevalainen and Dodds, 1995).*

lated to the inherent scatter of measured values of fracture toughness also introduce difficulties in the correlative methodology. Furthermore, extension of this correlative approach within a 3-D framework still remains a open issue; each of these characterizing parameters derive from a two-dimensional viewpoint, i.e., J, Q, vary pointwise along a crack front. Extensions and applications within a fully 3-D framework to treat these crack front variations remain elusive, as does their integration into a systematic treatment of strong statistical effects on cleavage toughness in the DBT region.

3. PROBABILISTIC MODELING OF CLEAVAGE FRACTURE

3.1 Probabilistic Fracture Parameter: The Weibull Stress

There has recently been a surge of interest in analyzing and predicting material failure caused by transgranular cleavage based upon a probabilistic interpretation of the fracture process. A

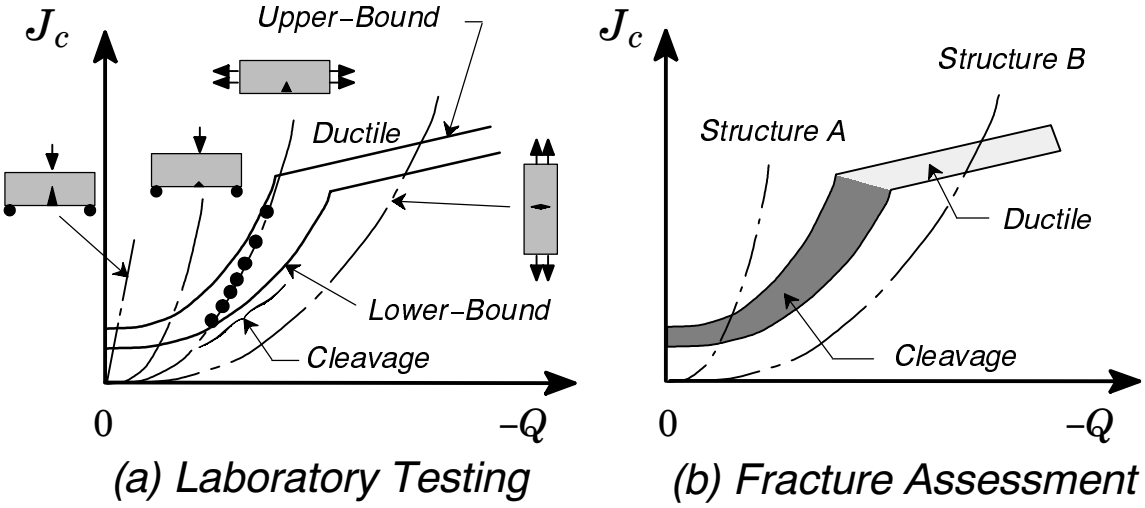

Figure 3 *Application of the J-Q methodology in fracture assessments (Dodds et al., 1993).*

primary impetus for bringing probabilistic fracture mechanics concepts into play is the inherent random nature of fracture due to inhomogeneity in the local characteristics of the material. The random character of fracture drives the development of probabilistic models employing weakest link arguments to describe the failure event. Such methodologies are collectively termed *local approaches* and couple the micromechanical features of the fracture process with the inhomogeneous distribution of the near-tip stress fields for multiaxially stressed, 3-D cracked bodies.

Limiting attention to the specific micromechanism of transgranular cleavage, Beremin (1983) has provided the basis for establishing a relationship between the microregime of fracture and macroscopic crack driving forces (such as the J-integral) by introducing the Weibull stress (σ_w) as a probabilistic fracture parameter. In Beremin's model, the probability distribution for the fracture stress of a cracked solid is a monotonically increasing function of loading (represented by the J-integral) given by the two-parameter Weibull distribution (Ruggieri and Dodds, 1996)

$$F(\sigma_w) = 1 - \exp\left[- \frac{1}{V_0} \int_{\Omega} \left(\frac{\sigma_1}{\sigma_u} \right)^m d\Omega \right] = 1 - \exp\left[- \left(\frac{\sigma_w}{\sigma_u} \right)^m \right] , \tag{5}$$

where Ω denotes the volume of the (near-tip) fracture process zone (FPZ), V_0 is a reference volume and σ_1 is the maximum principal stress acting on material points inside the FPZ additional details are found in related work by Ruggieri et al. (1996, 1997, 1999a, 1999b, 1999c). Ruggieri and Dodds (1996) define the FPZ as the loci $\sigma_1 \geq \lambda \sigma_0$, with $\lambda \approx 2$. Alternative definitions for the FPZ include the plastic region ahead of the macroscopic crack (Beremin, 1983; Mudry, 1987), $\sigma_e \geq \sigma_0$ where σ_e denotes the equivalent Mises stress. Parameters m and σ_u appearing in Eq. (5) denote the Weibull modulus and the scale parameter of the Weibull distribution. Following Beremin (1983), the Weibull stress is defined as the stress integral

$$\sigma_w = \left[\frac{1}{V_0} \int_{\Omega} {\sigma_1}^m d\Omega \right]^{1/m} . \tag{6}$$

In the context of probabilistic fracture mechanics, the Weibull stress, σ_w, emerges as a near-tip fracture parameter to describe the coupling of remote loading (as measured by J or, equivalently, K and CTOD) with a micromechanics model which incorporates the statistics of microcracks (weakest link philosophy). A key feature of this methodology is that σ_w incorporates

both the effects of stressed volume (the fracture process zone) and the potentially strong changes in the character of the near-tip stress fields due to constraint loss.

3.2 Toughness Scaling Methodology Using Weibull Stress Trajectories

Ruggieri and Dodds (1996) proposed a *toughness scaling model* to assess the combined effects of constraint variations on cleavage fracture toughness data. A central feature of this methodology lies on the interpretation of σ_w as the *crack tip driving force* coupled with the simple axiom that cleavage fracture occurs when the Weibull stress reaches a critical value, $\sigma_{w,c}$. For the same material at a fixed temperature, the scaling model requires the attainment of a specified value for the Weibull stress to trigger cleavage fracture in different specimens even though J-values may differ widely. In the probabilistic context adopted here, attainment of equivalent values of Weibull stress in different cracked configurations implies the same *probability* for triggering cleavage fracture.

Figure 4(a) illustrates the procedure to assess the effects of constraint loss on toughness values for different cracked configurations. The procedure employs J as the measure of macroscopic loading, but remains valid for other measures of remote loading, such as K_J or CTOD. Very detailed, nonlinear 3-D finite element analyses provide the functional relationship between the Weibull stress (σ_w) and applied loading (J) for a specified value of the Weibull modulus, m. The procedure illustrated in Fig. 4 aims to predict the (distribution of) fracture toughness values for configurations exhibiting low levels of crack-tip stress triaxiality, such as shallow notch SE(B) specimens (configuration B), from the measured toughness values obtained using high constraint, deep notch specimens, SE(B) or C(T) specimens (configuration A). Given the J_A-value for the high constraint fracture specimen, the lines shown on Fig. 4(a) readily illustrate the technique used to determine the corresponding J_B-value. Toughness values are often normalized by $b\sigma_0$ to provide a set of curves applicable for geometrically scaled specimens, i.e., all SE(B)s with $a/W = 0.5$, $W = B$, $S = 4W$.

3.3 LSY → SSY Constraint Corrections for Standard SE(B) Specimens

To illustrate an application of the Weibull stress based scaling model, Fig. 4(b) provides the constraint corrections (LSY → SSY) for a 1(T) SE(B) specimen with the material's elastic-plastic response described by a power hardening law given by $\epsilon/\epsilon_0 \propto (\sigma/\sigma_0)^n$ [see Ruggieri et al. (1999a, 1999b, 1999c)] for additional details) and for varying Weibull moduli, m. Here, the strain hardening exponent is $n = 10$ and $E/\sigma_0 = 500$ where E is Young's modulus and σ_0 denotes a reference (yield) stress; these values represent typical material response for pressure vessel steels. The LSY → SSY constraint corrections shown in the plots utilize the same methodology outlined in Fig. 4(a), but with curves of σ_w *vs.* J for the fracture specimen (configuration B) and for a plane-strain, SSY reference solution ($T/\sigma_0 = 0$) (configuration A) with the *same thickness of the fracture specimen*. Such curves are constructed for a fixed, representative value of the Weibull modulus, m, for the prescribed set of mechanical flow properties (the normalizing volume for the Weibull stress, V_0, is conveniently assigned the value of 1 mm^3). The present computations consider values of $m = 10$, 15, 20, 25 and 30 to assess the sensitivity of constraint corrections on the specified Weibull modulus. These m-values are consistent with previously reported values for structural steels.

Each curve displayed on Fig. 4(b) provides pairs of J-values, J_{LSY} in the SE(B) specimen and J_{SSY} in SSY, that produce the same σ_w. Reference lines are shown which define a constant ratio of "constraint loss", e.g., $J_{avg} = 1.2 \times J_0$ which implies that the SE(B) average J must be 20% larger than the SSY value to generate the same Weibull stress. For each value of the Weibull modulus, the SE(B) and SSY curves agree very well early in the loading history while the SE(B) specimen maintains near SSY conditions across the crack front (recall that computation of σ_w in the SE(B) specimens considers the entire crack front). Once near-front stresses deviate from the (plane-strain) SSY levels, the σ_w curves for the SE(B) specimens fail to increase at the same rate with further loading. These results illustrate clearly the gradual nature of constraint loss in the deep-notch SE(B) specimens, especially for moderate to low hardening

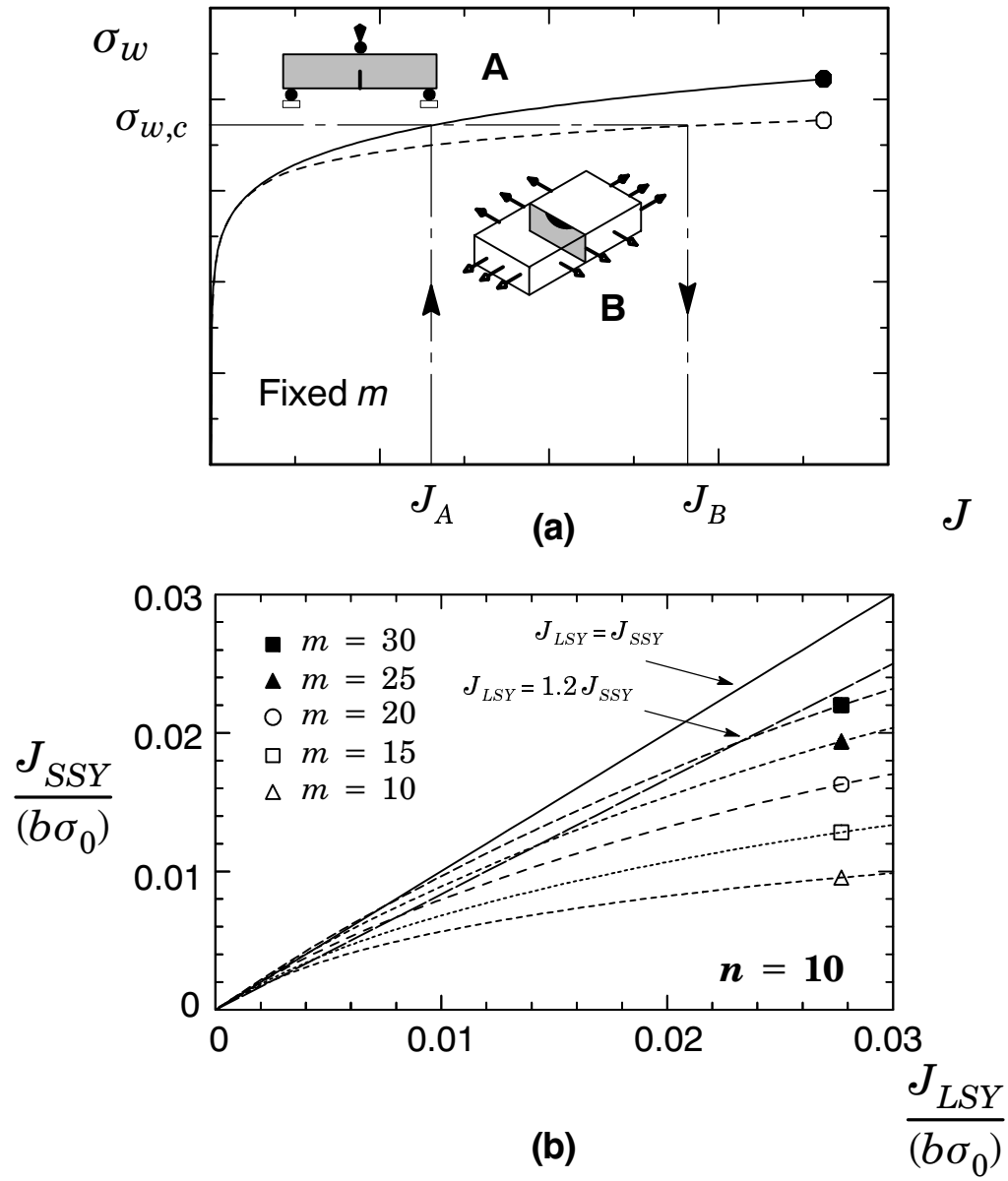

Figure 4 *(a) Toughness scaling model used to constraint correct toughness values for different crack configurations; (b)$J_{LSY} \rightarrow J_{SSY}$ correction for plane-sided 1(T) SE(B) specimens with n = 10.*

materials. The Weibull modulus does have an appreciable effect on predictions of constraint loss; increasing m values indicate a higher load level at the onset of constraint loss and a reduced rate of constraint loss under further loading. The larger m values, in effect, assign a greater weight factor to stresses at locations very near the crack front. The bending field, which impinges on the crack front, affects the smaller m curves more readily.

4. CONCLUDING REMARKS

The arguments presented in this brief paper, derived by extensive experimental observations, that conventional fracture mechanics approaches do not suffice to characterize the fracture behavior of fully yielded cracked solids provide compelling support to develop more realistic methodologies for fracture assessments. Our presentation explored the development of two recent of such methodologies. The *descriptive* approach employing multiparameter characterization of crack-tip fields relies on the J-Q theory. The *micromechanics* approach builds upon a probabilistic interpretation of the fracture process to yield a probabilistic fracture parameter termed

Weibull stress (σ_w). Unlike parameters derived from a descriptive methodology, such as the hydrostatic Q parameter, the Weibull stress provides a strong link between the microregime of fracture (by coupling a local failure criterion with the stresses that develop ahead of the macroscopic crack) and macroscopic (remote) loading (J). Recent on-going work has demonstrated the potential capability of the Weibull stress approach over the J-Q methodology to effectively *predict* constraint and ductile tearing effects in fracture specimens. Research efforts are in progress to refine the model and to establish a realistic, robust local approach for cleavage fracture.

Acknowledgements

This investigation was supported by grants principally from the Scientific Foundation of the State of São Paulo (FAPESP) under Grant 98/10574-2. Computational support provided by the High Performance Computing Center (LCCA) of the University of São Paulo is also aknowledged.

References

1. Toyoda, M., Minami, F., Matsuo, T., Hagiwara, Y and Inoue, T., "Effect of Work Hardening Properties of High Strength Steels on Cleavage/Ductile Fracture Resistance", Prep. National Meeting of the Japan Welding Society, Vol. 49, pp. 112–113, 1991 (in Japanese).
2. Wiesner, C. S. and Goldthorpe, M. R., "The Effect of Temperature and Specimen Geometry on the Parameters of the Local Approach to Cleavage Fracture" in *International Conference on Local Approach to Fracture (MECAMAT 96)*, Fontainebleau, France, 1996, pp. C6-295–304.
3. Larsson, S. G. and Carlsson, A. J., "Influence of Non–Singular Stress Terms and Specimen Geometry on Small Scale Yielding at Crack–Tips in Elastic–Plastic Materials", *Journal of the Mechanics and Physics of Solids*, Vol. 21, pp. 447–473, 1973.
4. Parks, D.M., "Advances in Characterization of Elastic–Plastic Crack–Tip Fields," in *Topics in Fracture and Fatigue,* A. S. Argon, Ed., Springer Verlag, pp. 59–98, 1992.
5. O'Dowd, N.P., and Shih, C.F., "Family of Crack–Tip Fields Characterized by a Triaxiality Parameter: Part I – Structure of Fields," *Journal of the Mechanics and Physics of Solids*, Vol. 39., No. 8, pp. 989–1015, 1991.
6. O'Dowd, N.P., and Shih, C.F., "Family of Crack–Tip Fields Characterized by a Triaxiality Parameter: Part II – Fracture Applications," *Journal of the Mechanics and Physics of Solids*, Vol. 40, pp. 939–963, 1992.
7. Dodds, R. H., Shih, C. F., and Anderson, T. L. "Continuum and Micro–Mechanics Treatment of Constraint in Fracture," *International Journal of Fracture*, Vol. 64, pp. 101–133, 1993.
8. Beremin, F.M, "A Local Criterion for Cleavage Fracture of a Nuclear Pressure Vessel Steel," *Metallurgical Transactions,* Vol. 14A, pp. 2277–2287, 1983.
9. Mann, N. R., Schafer, R. E. and Singpurwalla, N. D., *Methods for Statistical Analysis of Reliability and Life Data*, Jonh Wiley & Sons, New York, 1974.
10. Mudry, F., "A Local Approach to Cleavage Fracture", *Nuclear Engineering and Design*, Vol. 105, pp. 65–76, 1987.
11. Minami, F., Brückner–Foit, A., Munz, D.and Trolldenier, B., "Estimation Procedure for the Weibull Parameters Used in the Local Approach," *International Journal of Fracture*, Vol. 54, pp. 197–210, 1992.
12. Ruggieri, C., Minami, F. and Toyoda, M., "A Statistical Approach for Fracture of Brittle Materials Based on the Chain–of–Bundles Model", *Journal of Applied Mechanics*, Vol. 62, pp. 320–328, 1995.
13. Ruggieri, C. and Dodds, R. H., "A Transferability Model for Brittle Fracture Including Constraint and Ductile Tearing Effects: A Probabilistic Approach," *International Journal of Fracture*, Vol. 79, pp. 309-340, 1996.
14. Ruggieri, C. and Dodds, R. H., "WSTRESS Release 1.0: Numerical Computation of Probabilistic Fracture Parameters for 3-D Cracked Solids," *BT–PNV–30 (Technical Report)*, EPUSP, University of São Paulo, 1997.
15. Ruggieri, C., Dodds, R. H. and Wallin, K., "Constraints Effects on Reference Temperature, T_0, for Ferritic Steels in the Transition Region," *Engineering Fracture Mechanics*, Vol. 60, pp. 19-36, 1998.
16. Nevalainen, M. and Dodds, R. H., "Numerical Investigation of 3-D Constraint Effects on Brittle Fracture in SE(B) and C(T) Specimens," *International Journal of Fracture*, Vol. 74, pp. 131–161, 1995.
17. Williams, M.L., "On the Stress Distribution at the Base of a Stationary Crack", *Journal of Applied Mechanics,* Vol. 24, pp. 109–114, 1957.
18. Ruggieri, C., "A Framework to Correlate Effects of Constraint Loss and Ductile Tearing on Fracture Toughness – Part I: Probabilistic Approach," *15th Brazilian Congress of Mechanical Engineering (Cobem 99)*, Águas de Lindóia, Brazil (1999).
19. Ruggieri, C. and Trovato, E., "A Framework to Correlate Effects of Constraint Loss and Ductile Tearing on Fracture Toughness – Part II: Fracture Under Small Scale Yielding Conditions," *15th Brazilian Congress of Mechanical Engineering (Cobem 99)*, Águas de Lindóia, Brazil (1999).
20. Ruggieri, C., "A Framework to Correlate Effects of Constraint Loss and Ductile Tearing on Fracture Toughness – Part III: Parameter Calibration and Fracture Testing," *15th Brazilian Congress of Mechanical Engineering (Cobem 99)*, Águas de Lindóia, Brazil (1999).